

# A Novel Deep Learning Approach for Classification of COVID-19 Images

Malaya Kumar Nath  
Department of ECE  
NIT Puducherry  
Karaikal, India  
malaya.nath@nitpy.ac.in

Aniruddha Kanhe  
Department of ECE  
NIT Puducherry  
Karaikal, India  
aniruddhakanhe@nitpy.ac.in

Madhusudhan Mishra  
Department of ECE  
NERIST,  
Nirjuli, Arunachal Pradesh  
ecmadhusudhan@gmail.com

**Abstract**—Novel coronavirus 2019 (COVID-2019) initially started at Wuhan, China and spread all over the world and announced as pandemic by World Health Organization in March 2020. It makes use of all the available resources to reduce the disastrous effect of such Black Swan event. This virus causes pneumonia in human being and changes the respiratory pattern (different from common cold and flu). Compared to the reverse-transcription polymerase chain reaction (RT-PCR) chest X-ray and computed tomography imaging may be reliable and quick to diagnose the COVID-19 patients in the epidemic regions. Above mentioned imaging modalities along with the machine learning techniques can be helpful for accurate diagnosis of the disease and may be assistive in the absence of specialized physicians. Further, ML can improve throughput by accurate figuration of contagious X-ray and CT images for disease diagnosis, tracking and prognosis.

In this research, potential of artificial intelligence has been investigated to develop a deep neural network model for rapid, accurate and effective COVID-19 detection from the CT and X-ray images. The proposed method provides robust deep learning technique for binary (COVID vs. NON-COVID) and multi-class (COVID vs. NON-COVID vs. Pneumonia) classification from X-ray and CT images. A 24-layer CNN network has been proposed for the classification. It attains an accuracy of 99.68% and 71.81% on X-ray and CT images, respectively. For both the datasets Sgdm optimizer has been used with a learning rate 0.001.

**Index Terms**—COVID-19, CT, X-ray, Machine Learning, Convolutional Neural Network

## I. INTRODUCTION

The world has been facing global health challenge due to novel coronavirus-19 (COVID-19) disease, caused by severe acute respiratory syndrome [1]. Based on John Hopkins University data on 21 August 2020 there are 22,688,934 global confirmed cases including 793,773 deaths [2]. The number of conformed cases and death are highest in USA, Brazil, and India [3]. Government of various countries imposed restrictions on movement, social distancing, and creating awareness about hygiene. After June 2020 the spreading of virus occurs in an exponential manner. Infected person with COVID-19 virus experienced mild to moderate respiratory illness or pneumonia. The disease progress through three stages, such as: mild, severe, and critical [4]. No symptoms, mild coughing and fever are noticed in mild stage. More than 50% lung involvement in imaging along with dyspnea is visualized in severe stage. During critical condition, failure of multi organ and respiratory

system occurs and leads to death. Based on the data of National Center for Health Statistics (NCHS) the risk of severe illness is more than 50% in elder people (age more than 40) [5]. Person at any age having cancer, chronic kidney problem, cardiovascular disorder, persistent respiratory disease, type-2 diabetes, and sickle cell etc., are at increased risk for severe illness from COVID-19. A lot of clinical trials are ongoing all over the world for vaccine or potential treatment.

In order to fight against the spreading of corona virus effective and accurate screening and immediate medical attention to the infected person is a serious requirement. For identifying the COVID-19 affected people, reverse transcription polymerase chain reaction (RT-PCR) is adopted all over the world. This testing method is time consuming and suffers high value of false negative (FN) and false positive (FP) rates [6], [7]. Poor accuracy of RT-PCR may not be acceptable during rapid spreading period of the epidemic. Many countries are facing difficulties due to insufficient number of proper test kits. Delay in testing and inaccurate result may lead to community spread by the interaction of healthy individuals with the infected one.

Computed tomography (CT) and X-rays imaging of the chest can be utilized as an alternate to RT-PCR test for accurate diagnosis and various stages of disease evolution [8]. Easily available imaging techniques in all the hospitals of India may be the quicker and cheaper method for diagnosis of COVID-19. These radiography images of affected individuals have similar lesions [4], [9]. The most common pattern is ground glass opacity (GGO), which refers to the area of increased attenuation in lung with preserved bronchial and vascular markings. The GGO usually multifocal, bilateral, and peripheral. GGO may appear as unifocal lesion (found in the interior lobe of right lung) during the initial stage of the disease [9]. These imaging techniques produce a large amount of pathological images and needs detail analysis by the radiologist. Manual evaluation of the infection is tedious, tiresome, boring and also the influence of individual bias and clinical experience. Sometimes feature of COVID-19 being similar to viral pneumonia and lead to false diagnosis during overload condition. This leads to unnecessary utilization of healthcare resources.

Current technology make use of artificial intelligence (AI) to effectively handle healthcare issues and complications (such

as: breast cancer [10], skin cancer [11], glaucoma detection from retinal fundus image [12] & brain tumor detection [13], [14] etc.). Deep learning techniques have triggered much interest in its application to medical imaging domain as it reveals the detail image feature that are not possible from original images. Convolutional neural network (CNN) is found to be favourable in large group of research community. CNN is applied for classification and detection of various pathologies from radiograph images. Deep learning techniques are popular due its availability of the deep CNN network, which achieve good performance in some applications. This technique suffers due to the lack of large quantity training data. Transfer learning overcome the issue by utilizing the knowledge during training process and retrain the deep CNN with less number of data. Vikas et al., make use of this concept for pneumonia detection in chest X-ray images using a pre-trained model (such as: AlexNet, DenseNet121, InceptionV3, ResNet18, GoogleNet) on ImageNet dataset [15]. AlexNet and GoogLeNet have been used by Lakhani et al., to identify the pulmonary TB or normal [16]. In this research work chest images (Normal, Pneumonia affected and COVID-19 infected people) have been used by a proposed 24-layer CNN to classify the infected person. Classification result has been obtained for various optimizer and learning rate. This proposed CNN network achieved higher accuracy compared to the method presented in the literature. Rest part of the paper is organized as follows. Methodology for classification of COVID-19 is discussed in Section II. Experimental outcomes are presented in Section III. Finally, Section IV summarizes the work and presents a roadmap for future directives.

## II. METHODOLOGY COVID-19 CLASSIFICATION

A 24-layer CNN architecture consists of six convolution layer, has been proposed for classification of chest images infected by COVID-19. All the input images are resized to  $256 \times 256$  before feeding into the network for making the computation faster. Two filter sizes  $3 \times 3$  and  $5 \times 5$  have been used for convolution. ReLU activation function is used for non linearity, after the batch normalization (BN). ReLU does not saturate and the gradient remains high always. BN standardizes the input to a layer for each mini batch and accelerate the training process. It reduces the number of epoch by stabilizing the learning process. Max pooling uses a filter size of  $2 \times 2$  and shortens the computation time by cutting down the spatial dimension. It does not contribute to learning. The result of last pooling process fed to the fully connected layer for final classification. Then softmax is used just before the output layer, which assigns probabilities to each class. The general structure of the proposed CNN network is represented in Table I.

## III. EXPERIMENTAL OUTCOMES

In this study, two different schemes are studied for classification of COVID-19 and Normal images using different pre-trained model and the proposed CNN network. Various publicly available datasets are used for this study. The description

TABLE I  
GENERAL STRUCTURE AND PARAMETERS OF PROPOSED ARCHITECTURE

Type	Stride	Filter Size	Output Size
Input	-	-	$256 \times 256 \times 1$
Convolution1	1	$3 \times 3 \times 1 \times 16$	$254 \times 254 \times 16$
BN1	-	-	$254 \times 254 \times 16$
ReLU1	-	-	$254 \times 254 \times 16$
Max pooling1	2	-	$127 \times 127 \times 16$
Convolution2	1	$3 \times 3 \times 16 \times 32$	$125 \times 125 \times 32$
BN2	-	-	$125 \times 125 \times 32$
ReLU2	-	-	$125 \times 125 \times 32$
Max pooling2	-	-	$62 \times 62 \times 32$
Convolution3	1	$3 \times 3 \times 32 \times 64$	$60 \times 60 \times 64$
BN3	-	-	$60 \times 60 \times 64$
Convolution4	1	$3 \times 3 \times 64 \times 128$	$58 \times 58 \times 128$
BN4	-	-	$58 \times 58 \times 128$
ReLU4	-	-	$58 \times 58 \times 128$
Max pooling4	2	-	$29 \times 29 \times 128$
Convolution5	1	$5 \times 5 \times 128 \times 128$	$25 \times 25 \times 128$
BN5	-	-	$25 \times 25 \times 128$
Convolution6	1	$5 \times 5 \times 128 \times 128$	$21 \times 21 \times 128$
BN6	-	-	$21 \times 21 \times 128$
ReLU6	2	-	$21 \times 21 \times 128$
Max pooling6	2	-	$10 \times 10 \times 128$
Fully connected	-	$2 \times 1280$	$1 \times 1 \times 2$
Softmax	-	-	$1 \times 1 \times 2$

about dataset are given in Subsection III-A. These datasets have less number of images, which may affect the proposed network accuracy for a large dataset. So, data augmentation is carried out to increase the number of images before feeding to the network. Training was performed with and without augmentation for different optimizers, learning rate, and epochs. For various hyper parameter different performance metrics are computed and discussed in Subsection III-B. The simulation is carried out in Matlab 2019b by 64 bit, 3.6 GHz, i7-7700 processor with 8GB RAM and 2GB NVIDIA GeForce GT1030 graphics card.

### A. Database

X-ray and computed tomography images of the human lung help the physicians for quick diagnosis the disease. A couple of CT and X-ray image databases are publicly available. Joseph Paul Cohen from the University of Montreal has first shared the COVID-19 database in the GitHub website [17], [18]. It contains total 910 number of X-rays and CT scans of COVID-19 along with MERS, SARS, and ARDS. The images are available in jpg file format with different dimensions. Jinyu Zhao and their co. have created a COVID-CT-dataset containing 349 COVID and 397 NON-COVID CT images from 216 patients [19].

A group of research team from Qatar University Doha, Qatar and the University of Dhaka, Bangladesh in association

with the medical practitioners from Pakistan and Malaysia created a database of chest X-rays images for COVID-19 affected persons along with Normal and Pneumonia people [20]. This is found at Kaggle website. It contains 219 COVID-19, 1341 Normal and 1345 viral Pneumonia chest X-rays images having dimension of 1024×1024 in portable network graphics (PNG) file format. It has three classes and more suitable for study of COVID-19.

Among these modalities CT images of the chest provide a three dimensional picture of the chest lung from the slices. This helps to detect the sign of infection in the early stage of the disease and its nature in later stage. Analysis of the slices from CT images provide a qualitative evaluation to fight against COVID-19.

### B. Performance Metric

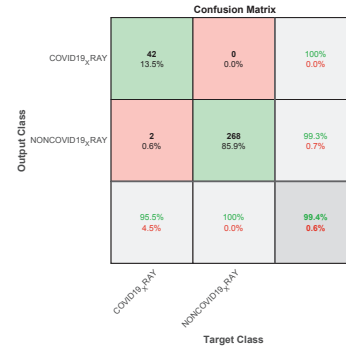
The performance of CNN is measured by accuracy, precision, sensitivity, specificity and dice similarity coefficient (DSC) [21]. For any class, they can be defined in Equation 1. The class is COVID-19 and Normal for a two class problem; COVID-19, Normal and Common flu infection (Pneumonia) in multi-class. True positive (TP) and true negative (TN) represent correctly classified COVID-19 and NON COVID-19 images, respectively. Wrongly detected samples are represented as false negative (FN) and false positive (FP), respectively. The performance values are ranging from 0 to 1. The metric value of these measures should lie close to '1' for better classification. F1-score can be computed from precision and sensitivity. It measures the test accuracy. F1-score value is identical to DSC measure. The performance metric are computed for two class (COVID-19 vs. Normal) and multi-class (COVID-19 vs. Normal Vs, Pneumonia) classification.

$$\begin{aligned}
 Accuracy &= \frac{TP + TN}{TP + TN + FP + FN} \\
 Precision &= \frac{TP}{TP + FP} = \text{Positive Predictive Value} \\
 Sensitivity &= \frac{TP}{TP + FN} = \text{Recall} \\
 Specificity &= \frac{TN}{TN + FP} \\
 DSC &= \frac{2 \times TP}{2 \times TP + FP + FN} \\
 F1 - score &= 2 \times \frac{Precision \times Sensitivity}{Precision + Sensitivity}
 \end{aligned} \tag{1}$$

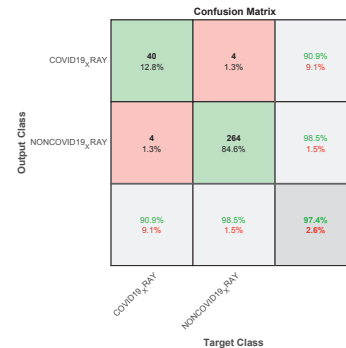
### C. Results: Two class (COVID-19 and Normal) problem

Classification performance of the proposed CNN architecture for two class (COVID-19 and Normal) is given in Table III. This result is obtained for X-ray images taken from Kaggle database [20]. Out of 219 (COVID) and 1341 (Normal) images, 80% from both the class are used for training. Rest 20% of the images are used for testing. The experiment is conducted for different optimizers (Sgdm, Adam, and RmsProp), epochs (5, 10, and 15) and learning rate (0.1, 0.01, and 0.001). All the optimizer recorded higher accuracy for in learning rate

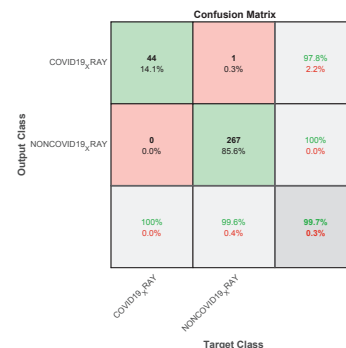
0.001. This value is found to be 99.68%, 99.68%, and 99.40% for Sgdm, Adam, and RmsProp optimizer, respectively. In all the optimizers accuracy value increases with lower learning rate and higher epoch. A decline trend is seen if the epoch is increased beyond certain value. This may occur due to over fitting. Highest F1-score (98.88%) is observed for Adam optimizer. This is achieved with 5 epochs and 0.001 learning rate. Figure 1 shows the confusion matrix for the testing images (44 COVID and 268 NON-COVID), for Adam, RmsProp and Sgdm optimizers.



(a)



(b)



(c)

Fig. 1. Confusion matrix for classification of X-ray images by the proposed CNN without augmentation with learning rate = 0.001, validation frequency = 2 for various optimizers: (a) Adam, (b) RmsProp, and (c) Sgdm.

TABLE II  
PERFORMANCE METRIC FOR X-RAY IMAGES: PROPOSED CNN FOR DIFFERENT OPTIMIZER (80% TRAINING AND 20% TESTING)

Optimizer	Learning rate	Epoch	Accuracy	Precision	Sensitivity	Specificity	DSC	F1-score
Sgdm	0.1	5	89.42	86.67	29.55	99.25	44.07	44.07
		10	87.82	54.17	88.64	87.69	67.24	67.24
		15	94.87	79.17	86.36	96.27	82.61	82.61
	0.01	5	97.12	90.70	88.64	98.51	89.66	89.66
		10	96.79	85.42	93.18	97.39	89.13	89.13
		15	97.44	86.00	97.73	97.39	91.49	91.49
	0.001	5	98.72	95.45	95.45	99.25	95.45	95.45
		10	<b>99.68</b>	97.78	100	99.63	<b>98.88</b>	98.88
		15	98.39	100	88.64	100	93.98	93.98
Adam	0.1	5	88.46	100	18.18	100	30.77	30.77
		10	96.15	100	72.73	100	84.21	84.21
		15	98.4	95.35	93.18	99.25	94.25	94.25
	0.01	5	97.12	90.70	88.64	98.51	89.66	89.66
		10	99.68	100	97.73	100	98.85	98.85
		15	98.08	97.50	88.64	99.63	92.86	92.86
	0.001	5	<b>99.68</b>	97.78	100	99.63	98.88	<b>98.88</b>
		10	99.36	100	95.45	100	97.67	97.67
		15	99.36	95.65	100	99.25	97.78	97.78
RmsProp	0.1	5	96.2	84.78	88.64	97.39	86.67	86.67
		10	96.79	97.22	79.55	99.63	87.50	87.50
		15	56.41	12.90	36.36	59.70	19.05	19.05
	0.01	5	95.34	78.43	90.91	96.04	84.21	84.21
		10	96.47	92.31	81.82	98.88	86.75	86.75
		15	98.08	93.18	93.18	98.88	93.18	93.18
	0.001	5	<b>99.36</b>	100	95.45	100	97.67	<b>97.67</b>
		10	97.44	90.91	90.91	98.51	90.91	90.91
		15	99.04	97.67	95.45	99.63	96.55	96.55

TABLE III  
PERFORMANCE METRIC CT IMAGES: PROPOSED CNN FOR DIFFERENT OPTIMIZER (80% TRAINING AND 20% TESTING)

Optimizer	Learning rate	Epoch	Accuracy	Precision	Sensitivity	Specificity	DSC	F1-score
Sgdm	0.001	10	<b>71.81</b>	68.92	72.86	70.89	70.83	70.83
Adam	0.001	5	61.07	65.00	37.14	82.28	47.27	47.27
RmsProp	0.001	5	56.4	51.91	97.14	20.25	67.66	67.66

To check the accurateness of classification of the proposed network augmented data is used. Here, number of images in the dataset are increased by rotation operation for all the classes before feeding into the network. Total 19980 augmented images (6570 COVID and 13410 NON-COVID) are fed to the network for classification. Accuracy of 99.64% is obtained for the Adam optimizer with learning rate of 0.001.

The same CNN network is used for CT images taken from [19]. For 0.001 learning rate highest accuracy 71.81% is obtained by Sgdm optimizer. The proposed network attains an accuracy of 61.07% and 56.4% for Adam and RmsProp optimizers, respectively. The classification performance in CT images is tabulated III. Accuracy is recorded to be less. This

may be due to the non availability of features in the slices, which is present in COVID class. This may also be applicable to the NON-COVID class. It may be due to the initial stage of the disease and features may not be prominent in any of the slices CT images.

#### D. Results: Multi-class (COVID-19, Normal, and Pneumonia) problem

The classification performance of the proposed CNN architecture for multi-class (COVID-19, Normal and Pneumonia) is computed for the X-ray images. Out of 581 test data (44 COVID, 268 NON-Covid, and 269 Pneumonia), 560 numbers (43 COVID, 254 NON-COVID, and 263 Pneumonia) are cor-

rectly classified. Here, Adam optimizer is used for 25 epochs and 0,001 learning rate. Individual classification accuracy of COVID, NON-COVID and Pneumonia are found to be 97.7%, 94.8% and 97.8%, respectively. Figure 2 shows the confusion matrix for multi-class classification from the X-ray images for Adam, RmsProp and Sgdm optimizer. Learning rate 0.001 is used. Accuracies of 96.4%, 95.4% and 95.5% are recorded for Adam, Sgdm and RmsProp optimizer, respectively.

**Confusion Matrix**

Output Class	COVID19_X_RAY	NONCOVID19_X_RAY	Viral Pneumonia	
COVID19_X_RAY	43 7.4%	2 0.3%	1 0.2%	93.5% 6.5%
NONCOVID19_X_RAY	0 0.0%	254 43.7%	5 0.9%	98.1% 1.9%
Viral Pneumonia	1 0.2%	12 2.1%	263 45.3%	95.3% 4.7%
	97.7% 2.3%	94.8% 5.2%	97.8% 2.2%	96.4% 3.6%
	COVID19_X_RAY	NONCOVID19_X_RAY	Viral Pneumonia	Target Class

(a)

**Confusion Matrix**

Output Class	COVID19_X_RAY	NONCOVID19_X_RAY	Viral Pneumonia	
COVID19_X_RAY	41 7.1%	0 0.0%	2 0.3%	95.3% 4.7%
NONCOVID19_X_RAY	0 0.0%	261 44.9%	15 2.6%	94.6% 5.4%
Viral Pneumonia	3 0.5%	7 1.2%	252 43.4%	96.2% 3.8%
	93.2% 6.8%	97.4% 2.6%	93.7% 6.3%	95.4% 4.6%
	COVID19_X_RAY	NONCOVID19_X_RAY	Viral Pneumonia	Target Class

(b)

**Confusion Matrix**

Output Class	COVID19_X_RAY	NONCOVID19_X_RAY	Viral Pneumonia	
COVID19_X_RAY	40 6.9%	0 0.0%	2 0.3%	95.2% 4.8%
NONCOVID19_X_RAY	1 0.2%	261 44.9%	13 2.2%	94.9% 5.1%
Viral Pneumonia	3 0.5%	7 1.2%	254 43.7%	96.2% 3.8%
	90.9% 9.1%	97.4% 2.6%	94.4% 5.6%	95.5% 4.5%
	COVID19_X_RAY	NONCOVID19_X_RAY	Viral Pneumonia	Target Class

(c)

Fig. 2. Confusion matrix for multi-class classification of X-ray images by the proposed CNN without augmentation with learning rate = 0.001, validation frequency = 10 for various optimizers: (a) Adam, (b) Sgdm, and (c) RmsProp.

## IV. CONCLUSIONS

In this paper, a novel 24-layer CNN architecture is proposed for classifying the COVID-19 from Normal and Pneumonia images. The network is tested on publicly available CT and X-ray images of the chest. Proposed CNN network attains an accuracy of 99.68% and 71.81% for X-ray and CT database (without augmentation) for two classes. Classification accuracy of X-ray images in proposed CNN architecture is better compared to the methods mentioned in the literature. This network attains 99.64% accuracy with augmentation. For multi-class an accuracy of 96.4% is recorded. Performance of classification in CT images can be improved with preprocessing, which may help to capture the feature in infected images.

## ACKNOWLEDGMENT

This work has been carried out in the ECE department of NIT Puducherry.

## REFERENCES

- [1] C. Wang, P. W. Horby, F. G. Hayden, and G. F. Gao, "A novel coronavirus outbreak of global health concern," *Lancet*, vol. 395, no. 10223, pp. 470–473, February, [https://doi.org/10.1016/S0140-6736\(20\)30185-9](https://doi.org/10.1016/S0140-6736(20)30185-9).
- [2] JHU, "COVID-19 dashboard by the center for system science engineering (CSSE) at John Hopkins University," *JHU*, accessed August 21, 2020, <https://coronavirus.jhu.edu/map.html>.
- [3] WHO, "Who coronavirus disease (COVID-19) dashboard," *WHO*, accessed August 21, 2020, <https://covid19.who.int/>.
- [4] R. Assistant, "COVID-19 imaging findings," *Radiology Assistant*, accessed August 21, 2020, <https://radiologyassistant.nl/chest/covid-19/covid19-imaging-findings>.
- [5] "People with certain medical conditions," accessed August 21, 2020, <https://www.cdc.gov/coronavirus/2019-ncov/need-extra-precautions/people-with-medical-conditions.html>.
- [6] A.-R. Ingrid, B.-G. Diana, S.-R. Daniel, Z.-A. Paula, del Campo Rosa, C. Agustin, S. Omar, M.-G. Laura, R. Anne, L. Nicola, B. P. M., P.-M. J. A, and Z. Javier, "False-negative results of initial RT-PCR assays for COVID-19: A systematic review," *medRxiv*, 2020. [Online]. Available: <https://www.medrxiv.org/content/early/2020/08/13/2020.04.16.20066787>
- [7] W. Shuai, K. Bo, M. Jinlu, Z. Xianjun, X. Mingming, G. Jia, C. Mengjiao, Y. Jingyi, L. Yaodong, M. Xiangfei, and X. Bo, "A deep learning algorithm using CT images to screen for corona virus disease (COVID-19)," *medRxiv*, 2020, <https://www.medrxiv.org/content/early/2020/04/24/2020.02.14.20023028>.
- [8] F. Shi, J. Wang, J. Shi, Z. Wu, Q. Wang, Z. Tang, K. He, Y. Shi, and D. Shen, "Review of artificial intelligence techniques in imaging data acquisition, segmentation and diagnosis for COVID-19," *IEEE Reviews in Biomedical Engineering*, pp. 1–1, 2020.
- [9] S. Salehi, A. Abedi, S. Balakrishnan, and A. Gholamrezanezhad, "Coronavirus disease 2019 (COVID-19): A systematic review of imaging findings in 919 patients," *American Journal of Roentgenology*, vol. 215, pp. 87–93, July 2020, <https://www.ajronline.org/doi/full/10.2214/AJR.20.23034>.
- [10] L. Shen, L. R. Margolies, J. H. Rothstein, E. Fluder, R. McBride, and W. Sieh, "Deep learning to improve breast cancer detection on screening mammography," *Scientific Reports*, 2019, <https://doi.org/10.1038/s41598-019-48995-4>.
- [11] D. Keerthana and M. K. Nath, "A technical review report on deep learning approach for skin cancer detection and segmentation," in *Springer Lecture Notes on Data Engineering and Communications Technologies*, Springer, Ed. Jan Wzykowski University, Poland and B.M. Institute of Engineering and Technology, India, June 2020, international Conference on Data Analytics and Management (ICDAM-2020).
- [12] P. Elangovan and M. K. Nath, "Glaucoma assessment from color fundus images using convolutional neural network," *International Journal of Imaging Systems and Technology*, 2020, <https://doi.org/10.1002/ima.22494>.

- [13] S. A. A. Ismael, A. Mohammed, and H. Hefny, "An enhanced deep learning approach for brain cancer MRI images classification using residual networks," *Artificial Intelligence In Medicine*, 2019, <https://doi.org/10.1016/j.artmed.2019.101779>.
- [14] M. Mittal, L. M. Goyal, S. Kaur, I. Kaur, A. Verma, and D. J. Hemanth, "Deep learning based enhanced tumor segmentation approach for MR brain images," *Applied Soft Computing Journal*, 2019, <https://doi.org/10.1016/j.asoc.2019.02.036>.
- [15] V. Chouhan, S. K. Singh, A. Khamparia, D. Gupta, P. Tiwari, C. Moreira, and V. H. C. D. A. Robertas Damaevius, "A novel transfer learning based approach for pneumonia detection in chest X-ray images," *Applied Sciences*, 2020, <https://doi.org/10.3390/app10020559>.
- [16] P. Lakhani and B. Sundaram, "Deep learning at chest radiography: Automated classification of pulmonary tuberculosis by using convolutional neural networks," *Radiology*, 2017, <https://doi.org/10.1148/radiol.2017162326>.
- [17] J. P. Cohen, P. Morrison, and L. Dao, "COVID-19 image data collection," *arXiv 2003.11597*, accessed August 20, 2020, <https://github.com/ieee8023/covid-chestxray-dataset>.
- [18] J. P. Cohen, P. Morrison, L. Dao, K. Roth, T. Q. Duong, and M. Ghassemi, "COVID-19 image data collection: Prospective predictions are the future," *arXiv 2006.11988*, accessed August 20, 2020, <https://github.com/ieee8023/covid-chestxray-dataset>.
- [19] J. Zhao, Y. Zhang, X. He, and P. Xie, "COVID-CT-dataset: a CT scan dataset about COVID-19," *arXiv preprint arXiv:2003.13865*, accessed August 20, 2020, <https://github.com/UCSD-AI4H/COVID-CT>.
- [20] A. K. T. Rahman, M. Chowdhury, "COVID-19 radiography database, kaggle," accessed August 20, 2020, <https://www.kaggle.com/tawsifurrahman/covid19-radiography-database/data>.
- [21] M. K. Nath, S. Dandapat, and C. Barna, "Automatic detection of blood vessels and evaluation of retinal disorder from color fundus images," *Journal of Intelligent and Fuzzy Systems IOS Press*, vol. 30, no. 5, pp. 6019–6030, May 2020, <https://doi.org/10.3233/JIFS-179687>.